Hernández-Uribe, D., and Tsujimori, T., 2023, Progressive lawsonite eclogitization of the oceanic crust: Implications for deep mass transfer in subduction zones: Geology, https://doi.org/10.1130/G51052.1

Supplemental Material

Supplemental Materials and Methods

Figures S1 and S2

Table S1

Supplemental Material for:

Progressive lawsonite eclogitization of the oceanic crust: Implications for deep mass transfer in subduction zones

David Hernández-Uribe[1*] and Tatsuki Tsujimori[2,3]

[1]Department of Earth and Environmental Sciences, University of Illinois Chicago, Chicago, Illinois 60607, USA

[2]Center for Northeast Asian Studies, Tohoku University, Sendai, Miyagi 980-8576, Japan

[3]Graduate School of Science, Tohoku University, Sendai, Miyagi 980-8578, Japan

MATERIALS AND METHODS

Modeling parameters

All phase calculations were performed using Theriak-Domino (de Capitani and Brown, 1987; de Capitani and Petrakakis, 2010) and the internally consistent thermodynamic data set ds62 (Holland and Powell, 2011) in the 10-component Na_2O–CaO–K_2O–FeO–MgO–Al_2O_3–SiO_2–H_2O–TiO_2–O_2 system. The following activity–composition relations for solid-solution phases were used: clinopyroxene ("omphacite model"), and clinoamphibole (Green et al., 2016); garnet, biotite, muscovite–paragonite, and chlorite (White et al., 2014); epidote (Holland and Powell, 2011); plagioclase (Holland and Powell, 2003); ilmenite (White et al., 2000).

Uncertainties related to the absolute positions of assemblage field boundaries on calculated phase diagrams have been shown to be less than ±1 kbar and ±50 °C at the 2σ level (Powell and Holland, 2008; Palin et al., 2016).

Whole-rock compositions

For calculations shown in Figures 1 and 2 in the main text, we use the normal mid-ocean ridge basalt (N-MORB) composition from Gale et al. (2013), the ocean island basalt (OIB) from Macdonald (1968), and the gabbro composition from White and Klein (2014) (Table S1). Individual phase diagrams for these lithologies are shown Figure S2. For models shown in Figures 3 and S1, we use the estimate of the altered mafic oceanic crust from Staudigel et al. (1996), the global estimate of the subducting sediments from Plank (2004), the mantle-wedge serpentinite from Deschamps et al. (2013) and the lawsonitite from Vitale-Brovarone and Beyssac (2014).

The bulk-rock X_{Fe}^{3+} [$X_{Fe}^{3+} = Fe^{3+}/(Fe^{2+}+Fe^{3+})$] ratios for all the whole-rock compositions were set to 0.24, lying within the range defined by fresh basaltic glasses, different sections of the fresh and altered oceanic crust, and exhumed mafic eclogites (0.10–0.36; Berry et al., 2018; Rebay et al., 2010; Walters et al., 2020).

Fluid in the models was considered to be pure H_2O. For the GLOSS, N-MORB, AOC, and OIB compositions, which are representative compositions of the uppermost portion of the oceanic crust, H_2O was set to ~4.5 wt% H_2O based on a mean of reported values from the literature relevant to the *P–T* conditions at the beginning of subduction (Hernández-Uribe and Palin, 2019 and references therein). The H_2O content for the gabbro was set to ~1.5 wt% based on modal mineralogy and seismic properties of the lower oceanic crust (Carlson, 2003). For the lawsonitite (Vitale-Brovarone and Beyssac, 2014), in order to account for the observed amount of lawsonite in such rock, the value of ~10.51 wt% (reported by Vitale-Brovarone and Beyssac,

2014) was used. Finally, the H_2O content for the mantle wedge serpentinite was set to ~10.81 wt%, which correspond to the reported value of Deschamps et al. (2013).

The ~4.5 wt% H_2O value lie well within in the range observed in lawsonite blueschist and eclogites (Whitney et al., 2020), whereas 1.5 wt% and the ~10–11 wt% are located in the lower and higher end, respectively, of the observed in natural lawsonite blueschist and eclogites (Whitney et al., 2020). For the calculations involving upper crustal composition, the ~4.5 wt% water content result in fluid excess through the *P*–*T* conditions considered herein. While basaltic rocks are mostly anhydrous, MORB and other lithologies in the upper oceanic crust are subject to hydrothermal alteration (Alt and Honnorez, 1984; Hernández-Uribe et al., 2020), supporting the used H_2O value is a reasonable estimate for the H_2O used in our models.

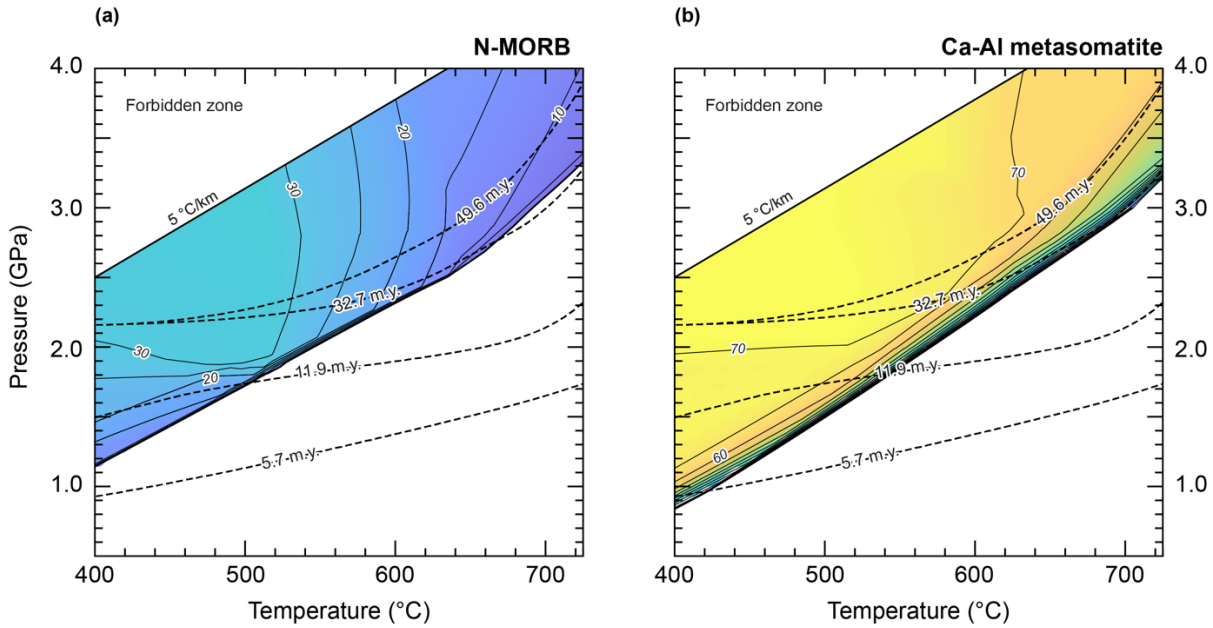

Figure S1. Pressure and temperature phase diagrams showing lawsonite stability for (a) N-MORB (as in Figure 1) and (b) the Ca-Al metasomatite. Both figures share the same color scale.

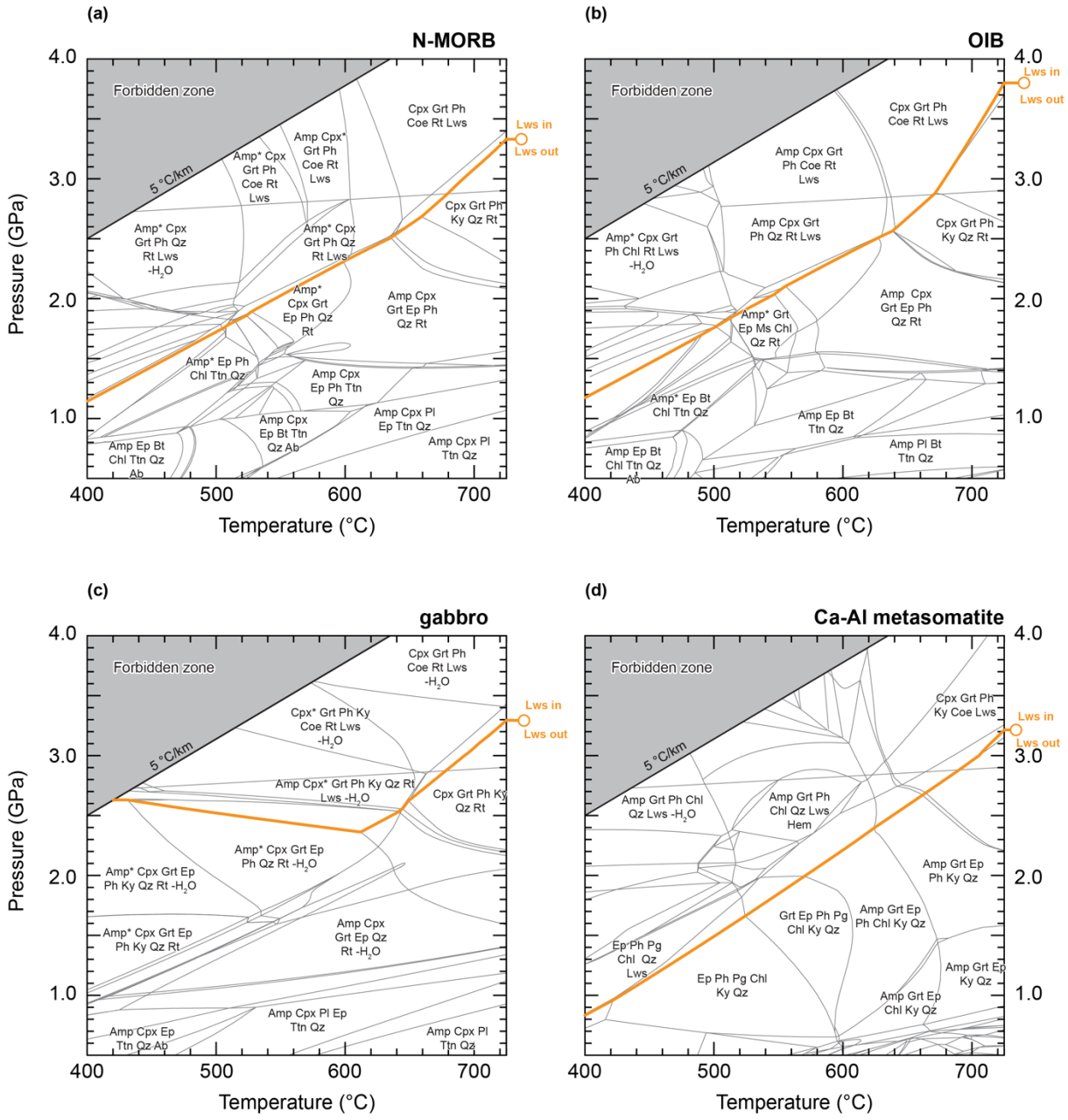

Figure S2. Pressure and temperature phase-equilibrium diagrams for all the considered lithologies. Mineral abbreviation follows Warr (2021). The asterisk in amphibole and clinopyroxene represent a solvi.

Table S1. Bulk-rock compositions used for phase equilibrium modeling (normalized mol%).

Sample	Figures	H_2O	SiO_2	Al_2O_3	CaO	MgO	FeO^{tot}	K_2O	Na_2O	TiO_2	O	Ca/Al	X_{Mg}
N-MORB	1, 2, 3	13.95	45.19	7.99	10.69	10.37	7.35	0.08	2.46	1.03	0.88	1.34	0.99
OIB	1	13.91	44.34	7.35	9.91	11.24	8.41	0.23	1.91	1.69	1.01	1.35	0.97
Gabbro	1	4.94	49.21	9.57	13.00	13.63	6.10	0.04	2.22	0.57	0.73	1.36	0.99
AOC	3	14.04	43.63	8.72	13.00	9.46	7.19	0.34	1.91	0.85	0.86	1.49	0.95
GLOSS	3	14.26	57.72	7.52	6.51	4.18	4.84	1.44	2.47	0.49	0.58	0.87	0.77
MWS	3	24.64	25.76	0.21	0.15	45.10	3.68	0.01	0.02	0.00	0.44	0.71	1.00
Ca-Al metasomatite	3, S1	30.19	33.62	13.57	12.36	5.59	4.14	0.02	0.03	0.00	0.50	0.91	1.00

FeO^{tot} is total iron expressed as FeO. Oxygen = O, which combines with FeO via the equation $2FeO + O = Fe_2O_3$; thus, bulk O is identically equal to bulk Fe_2O_3, while true bulk FeO is given by FeO^{tot}–2 X O. X_{Mg} = MgO/(MgO + FeO^{tot}), and $X_{Fe^{3+}}$ ratios = (2 X O)/FeO^{tot}

REFERENCES

Alt, J.C., and Honnorez, J., 1984, Alteration of the upper oceanic crust, DSDP site 417: mineralogy and chemistry: Contributions to Mineralogy and Petrology, v. 87, p. 149–169.

Berry, A.J., Stewart, G.A., O'Neill, H. S C., Mallmann, G., and Mosselmans, J.F.W., 2018, A re–assessment of the oxidation state of iron in MORB glasses: Earth and Planetary Science Letters, v. 483, p. 114–123.

Carlson, R.L., 2003, Bound water content of the lower oceanic crust estimated from modal analyses and seismic velocities of oceanic diabase and gabbro: Geophysical Research Letters, v. 30, p. 2142.

de Capitani, C., and Brown, T.H., 1987, The computation of chemical equilibrium in complex systems containing non-ideal solutions: Geochimica et Cosmochimica Acta, v. 51, p. 2639–2652.

de Capitani, C., and Petrakakis, K., 2010, The computation of equilibrium assemblage diagrams with Theriak/Domino software: American Mineralogist, v. 95, p. 1006–1016.

Deschamps, F., Godard, M., Guillot, S., and Hattori, K., 2013, Geochemistry of subduction zone serpentinites: A review: Lithos, v. 178, p. 96−127.

Gale, A., Dalton, C.A., Langmuir, C.H., Su, Y., and Schilling, J.G., 2013, The mean composition of ocean ridge basalts: Geochemistry, Geophysics, Geosystems, v. 14, 489−518.

Green, E.C.R., White, R.W., Diener, J.F.A., Powell, R., Holland, T.J.B., and Palin, R.M., 2016, Activity–composition relations for the calculation of partial melting equilibria in metabasic rocks: Journal of Metamorphic Geology, v. 34, p. 845−869.

Hernández-Uribe, D., and Palin, R.M., 2019, A revised petrological model for subducted oceanic crust: Insights from phase equilibrium modelling: Journal of Metamorphic Geology, v. 37, 745–768 (2019).

Holland, T.J.B., and Powell, R., 2003, Activity–composition relations for phases in petrological calculations: an asymmetric multicomponent formulation: Contributions to Mineralogy and Petrology, v. 145, p. 492–501.

Holland, T.J.B., and Powell, R., 2011, An improved and extended internally consistent thermodynamic dataset for phases of petrological interest, involving a new equation of state for solids: Journal of Metamorphic Geology, v. 29, p. 333–383.

Macdonald, G.A., 1968, Composition and origin of Hawaiian lavas. Geological Society of America Memoirs v. 116, p. 477–522.

Palin, R.M., Weller, O.M., Waters, D.J., and Dyck, B., Quantifying geological uncertainty in metamorphic phase equilibria modelling; a Monte Carlo assessment and implications for tectonic interpretations: Geoscience Frontiers, v. 7, p. 591–607.

Plank, T., 2014, The chemical composition of subducting sediments. Elsevier.

Powell, R., and Holland, T.J.B., 2008, On thermobarometry: Journal of Metamorphic Geology, v. 26, p. 155–179.

Rebay, G., Powell, R., and Diener, J.F.A., 2010, Calculated phase equilibria for a MORB composition in a P–T range, 450–650 C and 18–28 kbar: the stability of eclogite: Journal of Metamorphic Geology, v. 28, p. 635–645.

Staudigel, H., Plank, T., White, B., and Schmincke, H. U. Geochemical fluxes during seafloor alteration of the basaltic upper oceanic crust: DSDP Sites 417 and 418: Subduction: top to bottom, v. 96, p. 19–38.

Vitale-Brovarone, A., and Beyssac, O., 2014, Lawsonite metasomatism: A new route for water to the deep Earth: Earth and Planetary Science Letters, v. 393, p. 275–284.

Walters, J.B., Cruz-Uribe, A.M., and Marschall, H.R., 2020, Sulfur loss from subducted altered oceanic crust and implications for mantle oxidation. Geochemical Perspective Letters, v. 13, p. 36–41.

Warr, L. N., 2021, IMA–CNMNC approved mineral symbols: Mineralogical Magazine, v. 85, p. 291–320.

White, R. W., Powell, R. Holland, T.J.B., Johnson, T.E., and Green, E.C.R., 2014, New mineral activity–composition relations for thermodynamic calculations in metapelitic systems: Journal of Metamorphic Geology, v. 32, p. 261–286.

White, R. W., Powell, R., Holland, T. J. B. and Worley, B. A., 2000, The effect of TiO_2 and Fe_2O_3 on metapelitic assemblages at greenschist and amphibolite facies conditions: mineral equilibria calculations in the system K_2O–FeO–MgO–Al_2O_3–SiO_2–H_2O–TiO_2–Fe_2O_3: Journal of Metamorphic Geology, v. 18, p. 497–511.

White, W.M., and Klein, E.M., 2014, Composition of the oceanic crust: Treatise on Geochemistry (second edition), p. 457–496.

Whitney, D.L., Fornash, K.F., Kang, P., Ghent, E.D., Martin, L., Okay, A.I., and Vitale-Brovarone, A., 2020, Lawsonite composition and zoning as tracers of subduction processes: A global review: Lithos, v. 370, p. 105636.